Myocardial First Pass Perfusion: Steady-State Free Precession versus Spoiled Gradient Echo and Segmented Echo Planar Imaging

Yi Wang,[1,2]* Khurram Moin,[2,3] Olakunle Akinboboye,[2,3] and Nathaniel Reichek[2,3]

The imaging sequences used in first pass (FP) perfusion to date have important limitations in contrast-to-noise ratio (CNR), temporal and spatial resolution, and myocardial coverage. As a result, controversy exists about optimal imaging strategies for FP myocardial perfusion. Since imaging performance varies from subject to subject, it is difficult to form conclusions without direct comparison of different sequences in the same subject. The purpose of this study was to directly compare the saturation recovery SSFP technique to other more commonly used myocardial first pass perfusion techniques, namely spoiled GRE and segmented EPI. Differences in signal-to-noise ratio (SNR), CNR, relative maximal upslope (RMU) of signal amplitude, and artifacts at comparable temporal and spatial resolution among the three sequences were investigated in computer simulation, contrast agent doped phantoms, and 16 volunteers. The results demonstrate that SSFP perfusion images exhibit an improvement of approximately 77% in SNR and 23% in CNR over spoiled GRE and 85% SNR and 50% CNR over segmented EPI. Mean RMU was similar between SSFP and spoiled GRE, but there was a 58% increase in RMU with SSFP versus segmented EPI. Magn Reson Med 54:1123–1129, 2005.

Key words: myocardial first pass perfusion; contrast agent; pulse sequence; SNR; upslope

MR myocardial contrast first pass (FP) imaging can provide important information about regional myocardial perfusion. When combined with pharmacological stress test, it is a promising diagnostic tool for the assessment of ischemic heart disease (1,2).

The goal of MR myocardial FP is to image the early distribution of contrast agent in the myocardium at a high spatial and temporal resolution through bolus administration of a T_1-shortening contrast agent. Typically, multiple slices per heartbeat are acquired during first pass of the contrast through the myocardium, using T_1-weighted fast gradient echo sequences. Short TE, TR, and magnetization preparation are commonly utilized to increase tissue T_1 contrast in the myocardial region. Standard magnetization preparation includes slice-selective (3) or non-slice-selective (4) 90° saturation recovery (SR) (5) or 180° inversion recovery pulses (6,7). T_1 weighting and the rapid data acquisition requirement are usually met by incorporating gradient echo techniques. For example, spoiled GRE (TurboFLASH), a gradient echo technique with very short TR and TE, is one of the first T_1-weighted techniques applied in MR FP and most MR FP publications reported thus far are based on this imaging sequence (8). Segmented EPI, another gradient echo technique, uses an echo-train readout (9) to improve the temporal resolution. Instead of reading one frequency encoding line for every radiofrequency (RF) excitation pulse, segmented EPI reads two to four lines for each RF pulse by rapidly switching the readout gradient polarity. Thus, the data acquisition time is greatly reduced. However, both techniques suffered from suboptimal signal-to-noise ratio (SNR), especially if the scan duration is prolonged. Limited SNR also precludes consistent reproducibility of MR FP perfusion with either visual assessment or myocardial flow quantification. Although MR perfusion imaging has clear advantages over other modalities in terms of ease of use, being noninvasive, and having higher spatial resolution, it is currently not a standard clinical tool for assessment of ischemic disease. Improved SNR on perfusion images will likely enhance its success for clinical application. Recently, steady-state free precession (SSFP) techniques such as TrueFISP have been applied successfully to cardiac MR cine imaging and have demonstrated exceptional contrast between blood and myocardium (10). SSFP, as a coherent gradient echo technique, recycles the transverse magnetization for each data acquisition, unlike that of incoherent techniques that tend to spoil all the transverse magnetization. Preliminary research using the new SSFP perfusion technique (11) has been published and demonstrates higher SNR and/or better resolution in FP images (7,12). However, for FP imaging, unlike cine SSFP, the steady state of magnetization must be disturbed and re-established with every heartbeat because of the magnetization preparation pulse requirement to enhance the T_1 contrast in the myocardium. In our SSFP perfusion sequence, a set of dummy pulses was played prior to the actual data acquisition to establish the steady state (13) for each ECG triggering pulse. To better understand the SSFP perfusion mechanism and performance compared to other perfusion techniques, a systematic evaluation is needed. Some preliminary studies have been reported on this topic (11) (12), but no study has been done with the same resolution on the same subject, as described in this study.

[1]Research and Education Department, St. Francis Hospital, Roslyn, New York, USA.

[2]Department of Biomedical Engineering, SUNY at Stony Brook, Stony Brook, New York, USA.

[3]Department of Medicine, SUNY at Stony Brook, Stony Brook, New York, USA.

Presented at the Eleventh Annual Meeting and Exhibition of ISMRM, Toronto, Canada, July 2003.

*Correspondence to: Yi Wang, MRI Suite, DeMatteis Center, Research Department, St. Francis Hospital, Heart Center, 100 Port Washington Boulevard, Roslyn, NY 11576, USA. E-mail: yi.wang@chsli.org

Grant Sponsor: American Heart Association National Scientist Development; Grant Number: 0435311N; Grant Sponsor: Quest Diagnostics Foundation.

Received 27 January 2005; revised 5 July 2005; accepted 22 July 2005.

DOI 10.1002/mrm.20700

Published online 10 October 2005 in Wiley InterScience (www.interscience.wiley.com).

The purpose of this study was to directly compare the SSFP technique to other more commonly used myocardial first pass perfusion techniques, namely spoiled GRE and segmented EPI. We evaluated and compared signal behavior of saturation recovery SSFP, segmented EPI, and spoiled GRE perfusion images in computer simulations, contrast agent doped phantoms, and human subjects studied with multiple FP sequences at the same sitting with the same spatial resolution.

METHODS

Computer Simulations

In order to compare signal performance in various techniques, a computer model was created with the following equation to simulate MR signal from both SR SSFP and spoiled GRE sequence (14).

The signal for SR spoiled GRE sequence S_{TFL} can be expressed as

$$S_{\mathrm{TFL}} = M_0(1 - E1))(1 - \exp(-TI/T_1))\exp(-TE/T_2^*) * \sin\alpha/(1 - E1 * \cos\alpha). \quad [1]$$

The signal of saturation recovery SSFP sequence S_{TFL} is (15)

$$S_{\mathrm{TFI}} = M_0(1 - E1)(1 - \exp(-TI/T_1))\exp(-TE/T_2^*) * \sin\alpha/(1 - (E1 - E2) * \cos\alpha - E1 * E2), \quad [2]$$

where α is the RF flip angle, TI is the saturation time (the time between center of saturation pulse to that of data acquisition), and M_0 is the equilibrium magnetization; $E1 = \exp(-\mathrm{TR}/T_1)$ and $E2 = \exp(-\mathrm{TR}/T_2)$. The signal of SR segmented EPI sequence was not simulated separately because of its similar behavior as SR spoiled GRE in Eq. [1] (16). The effect of T_2/T_1 dependence of SR SSFP signal will be discussed later.

Contrast agent changes the apparent T_1, which should be inversely proportional to contrast agent concentration, as shown below:

$$1/T_1 - 1/T_{10} + R_1[\mathrm{Gd}], \quad [3]$$

where T_{10} is the tissue T_1 without contrast agent (all in seconds), [Gd] is the gadolinium concentration in millimoles per liter (mM), and R_1 is the longitudinal relaxivity of gadolinium chelate/(mmol/liter) · s. The R_1 for the contrast agent we used in all our experiments, Omniscan (Amersham, Princeton, NJ, USA), is 4.5 mmol/liter · s.

The first simulation was designed to verify the linear relation between the signal intensity and contrast concentration for our sequence and contrast agent dosages. A T_1 of 100 ms was used to mimic the contrast concentration of 2 mM in the ventricular blood pool, while a T_1 of 200–500 ms was used to mimic the concentration of the myocardium. Linear regression analysis was performed for both SR SSFP and spoiled GRE signal versus concentration curves.

Matlab software (The MathWorks, Inc., Natick, MA, USA) was used for simulation. In our model, TR/TE/TI = 3/1/90 ms, T_2 = 250 ms, T_2^* = 100 ms, flip angle was 50° for SSFP and 15° for spoiled GRE. Blood pool and myocardial signals for spoiled GRE and SSFP at different flip angles were simulated according to Eqs. [1] and [2], respectively.

Phantom Studies

We verified that signal intensity was inversely proportional to contrast agent concentration within the range of interest by all three sequences with parameters similar those used in human study on Gd-DTPA doped tubes (3 cm in diameter) with a smaller field of view and use of a head coil. To examine the relative signal intensity, receiver gain was kept the same for all sequences. Regions of interests (ROI) were drawn on each tube image obtained after signal reached steady state.

Tubes with varying contrast agent concentrations (Gd with saline solution) were used. The T_1 of each tube was estimated by using an inversion recovery spin echo sequence with a long TR. The estimated T_1 range of 90 to 1100 ms corresponded to concentrations ranging from 0.05 to more than 2 mM, according to Eq. [3]. ROIs were drawn across the whole cross section of tubes. Linear regression analysis was performed for each curve.

Volunteer Studies

Sixteen volunteers (38 to 73 years old, 5 females) without a clinical history of coronary artery disease underwent informed consent after enrollment in this study with institutional IRB approval. The study was performed on a 1.5 T Siemens Sonata scanner (Siemens Medical Solutions, Malvern, PA, USA) with a circular polarized body array flex coil and a gradient system capable of switching at 40 mT/m. First pass MR perfusion studies in each volunteer were performed with two pulse sequences in random order (spoiled GRE versus SSFP on 8 volunteers and segmented EPI versus SSFP on the other 8), with a 20-min washout period between contrast injections. First pass breath-hold perfusion imaging was obtained over 50 cardiac cycles with data acquisition starting 2 cardiac cycles prior to contrast agent administration.

The gadolinium-based contrast agent in MRI shortens T_1 relaxation and enhances myocardial signal on the saturation recovery MR images. Its effects depend on the dosage, rate of delivery, and distribution volume. Higher contrast concentration improves SNR, but only to a certain extent (17–19). Fast injection tightens the bolus, but the effect presents more clearly in the dynamic signal from left ventricle blood, not so much as in the myocardium. Ishida suggested 5 cc/s as a reasonable injection rate to use (20). We picked the same dosages (0.05 mmol/kg) and injection rate (6 cc/s) according to most clinical application published. According to our computer simulations, those parameters will keep image amplitude of all sequences in linear range.

Volunteers were instructed to hold their breath at the expiration as long as possible and to take shallow rapid breathes thereafter until data acquisition was complete. The i.v. contrast agent bolus was injected with a Spectris MR power injector (Medrad, Indianola, PA, USA) at a rate

of 6 mL/s and a half dose of (0.05 mmol/kg body wt) gadodiamide (Omniscan, Amersham, Nycomed, Princeton, NJ, USA). Breath-hold first pass perfusion imaging was obtained within 50 cardiac cycles with data acquisition starting 2 cardiac cycles prior to contrast agent administration.

The sequence parameters for the SR-SSFP were TR/TE/TI/FA = 2.6 ms/1 ms/90 ms/50°, raw data matrix of 60 × 128, rectangular field of view 21 × 34 cm^2, bandwidth (BW) per pixel 980 Hz, and voxel spatial resolution 3.5 × 2.6 × 8 mm^3. Four slices were acquired per RR interval (three short-axis slices from base to apex, one four-chamber-view long-axis slice). A separate saturation pulse was applied to each slice. Five dummy scans had been applied before real data acquisition started in order for the SSFP magnetization to reach equilibrium. For the SR-spoiled GRE pulse sequence, parameters were TR/TE/TI/FA = 2.4 ms/1 ms/90 ms/15°, pixel BW 850 Hz, and the same pixel resolution as used for SSFP. The acquisition time per image was the same with both sequences, 160 ms.

For comparison of SSFP and segmented EPI, partial *k*-space SSFP data were acquired (21). This technique utilizes the symmetric property of the *k*-space data to predict and interpolate all of *k*-space with only part of the *k*-space data in phase encoding direction. The parameters for SR-segmented EPI were as follows: TR/TE/TI/FA = 5.6 ms/1.17 ms/30 ms/30°, EPI factor = 4, 6–7 slices acquired per RR interval, and voxel spatial resolution was the same at 2.7 × 3.4 × 8 mm^3. The acquisition time per image was the same with both sequences, roughly 120 ms.

Data Processing

Siemens Argus software was used for SNR and CNR analysis. For SNR analysis, ROIs were placed in the left ventricular cavity and background, as well as the septum, lateral, anterior, and inferior wall from the last perfusion image at a time when the contrast signal in myocardium had stopped changing rapidly. SNR was calculated from the ratio of mean signal intensity in certain ROI and the SD of the signal intensity of a background ROI. A total of six circular ROIs (ventricular blood, background, and four in different area of myocardium) for each slice of any perfusion study were drawn within the myocardial contours as large as possible. For CNR analysis, ROIs were placed using mean curve at the similar locations on the images with peak contrast signal, as well as on the baseline image of the same perfusion series. The CNR was calculated from the difference of these two signals dividing by the background signal SD. The mean and SD of both SNR and CNR for all slices and all subjects were compared for each sequence pair.

MASS (Medis Medical Systems, Leiden, The Netherlands) software was used to plot myocardial signal intensity over time. Epicardial and endocardial contours were manually traced on an image from each slice with good contrast between blood pool and myocardium. The contours were then propagated through the whole perfusion series in that slice, with manual correction to compensate for respiratory motion when needed. The myocardium was clockwise divided equally into six segments, starting from the posterior atrioventricular node of septum, posterior septum, anterior septum, anterior wall, anterior lateral wall, lateral wall, and posterior wall. Signal from all pixels in each segment was averaged. Normalized signal intensities were obtained by dividing each value by the precontrast signal intensity to compensate for the surface coil induced penetration effects (details in Discussion and Conclusion). A dynamic signal upslope for each time point was calculated from four adjacent time points using a linear least squares fit. The maximal upslope for each myocardial segment was then identified. An ROI was also placed in the left ventricular cavity for each slice and a maximal upslope of the ventricular signal was calculated in the same fashion as in myocardium except with two adjacent time points used for fitting. To correct for differences in input function, the myocardial upslope was normalized by dividing the upslope of the left ventricular signal intensity curve. The final corrected upslope was termed the relative maximal upslope (RMU). To avoid variation from artifact and breathhold position change between two scans, the middle three slices were used to compare the RMU. Paired Student *t* test with two tails was used to analyze the results.

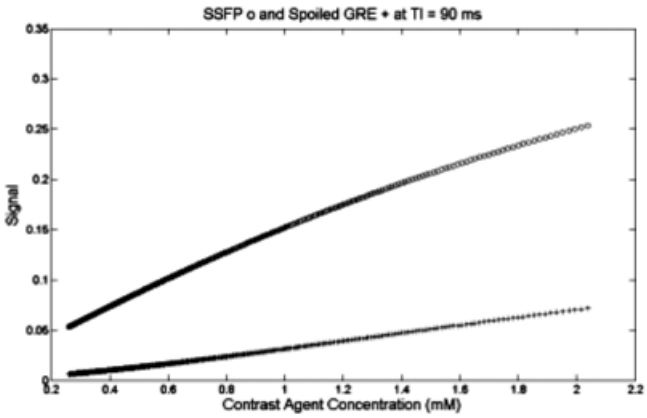

FIG. 1. Simulated saturation recovery SSFP and spoiled GRE signals versus contrast concentration (corresponding to T_1 from 500 to 100 ms).

RESULTS

Computer Simulations

Figure 1 shows the simulated signals from SSFP and spoiled GRE over T_1 from 100 to 500 ms (equivalent concentration 0.26 to 2.04 mmol/liter (or mM)) at saturation recovery time of 90 ms. T_1 of 100 ms was used to represent peak ventricular blood concentration of gadiomide, which is achievable with tight i.v. bolus contrast agent administration even at a relatively low contrast agent dosages. The SSFP signal was higher than the spoiled GRE signal, and this was even more marked when contrast concentration increased. Signals from both sequences are relatively linear with concentration change within the range. However, the SSFP signal started to show curve shape at high contrast concentration, while the spoiled GRE signal remains linear. A linear regression analysis of signal versus contrast concentration showed that R^2 was 0.99 and 1 for

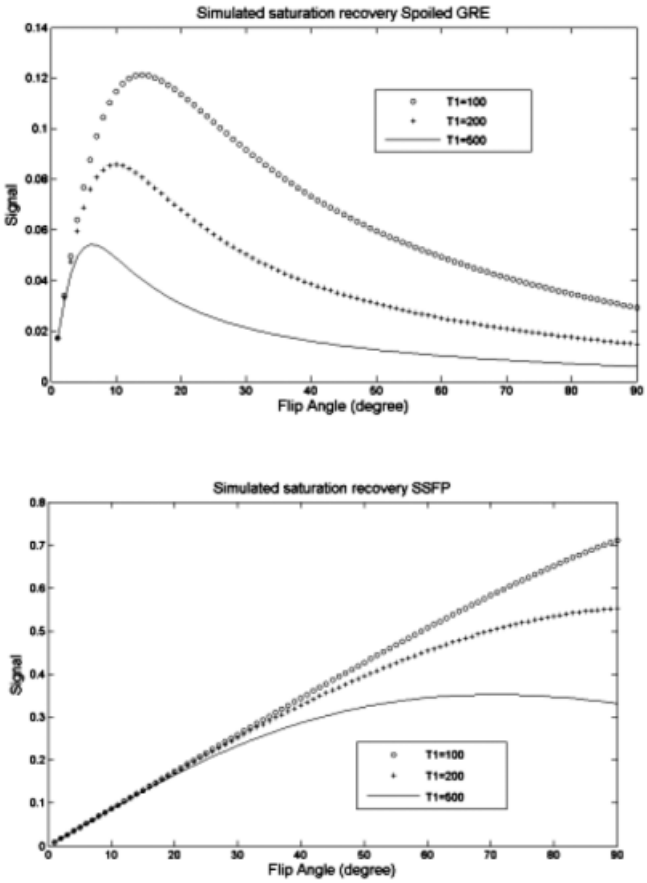

FIG. 2. Optimal flip angle for both saturation recovery spoiled GRE (upper) and SSFP (lower).

SSFP and spoiled GRE, respectively, with $P < 0.0001$ for all curves.

Figure 2 shows that the optimal flip angle varies with the T_1 or contrast concentration. For spoiled GRE, the optimal flip angle was between 15 and 20 ° under these conditions; SSFP uses a higher flip angle and yields better signal. Due to the SAR limitation, a flip angle of 50° was used in our SSFP perfusion studies.

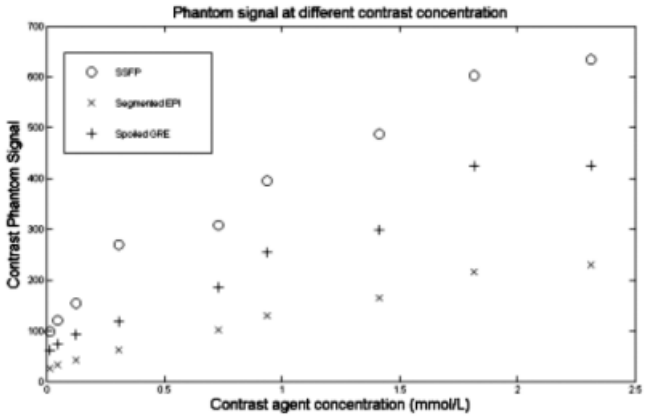

FIG. 3. Phantom signal with saturation recovery SSFP, segmented EPI, and spoiled GRE sequence versus different contrast concentration (corresponding to T_1 from 90 to 1100 ms).

Phantom Studies

Mean SSFP, segmented EPI, and spoiled GRE signal amplitudes of tube phantoms with different concentrations using parameters similar to those used in volunteer study are shown in Fig. 3. T_1 was determined using an inversion recovery spin echo sequence. As seen from the plot, signal from all three sequences follows the contrast concentration reasonably well. However, both absolute signal amplitude and the slope of signal amplitude against concentration are lowest with segmented EPI and highest with SSFP. A linear regression analysis of signal versus contrast concentration showed that R^2 was 0.96, 0.97, and 0.99 for SSFP, spoiled GRE, and segmented EPI, respectively, with $P < 0.0001$ for all curves.

Volunteer Studies

Perfusion images from all three sequences demonstrated reasonable quality with adequate contrast between myo-

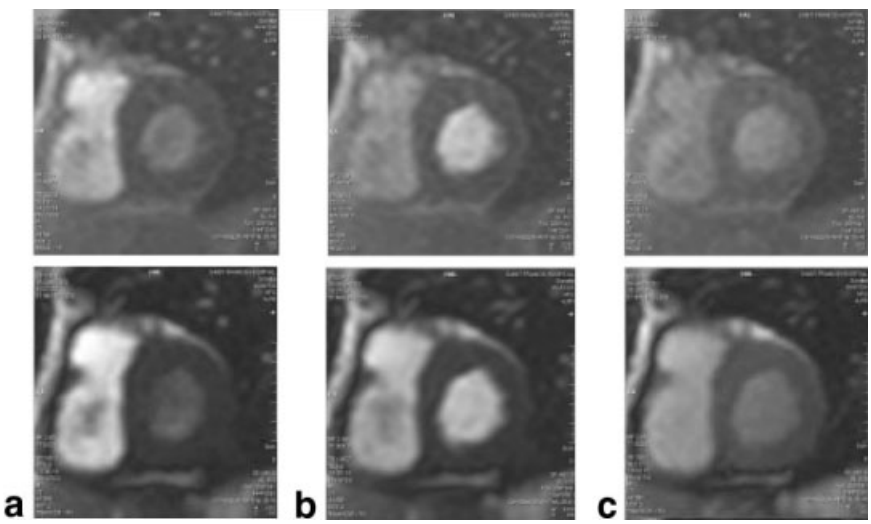

FIG. 4. Perfusion images when contrast agent reaches left ventricle (**a**), at maximal signal in left ventricle (**b**), and at maximal signal in myocardium (**c**) with spoiled GRE (upper panel) and SSFP (lower panel), respectively. In this case, spoiled GRE was used first, and SSFP was used 20 min later.

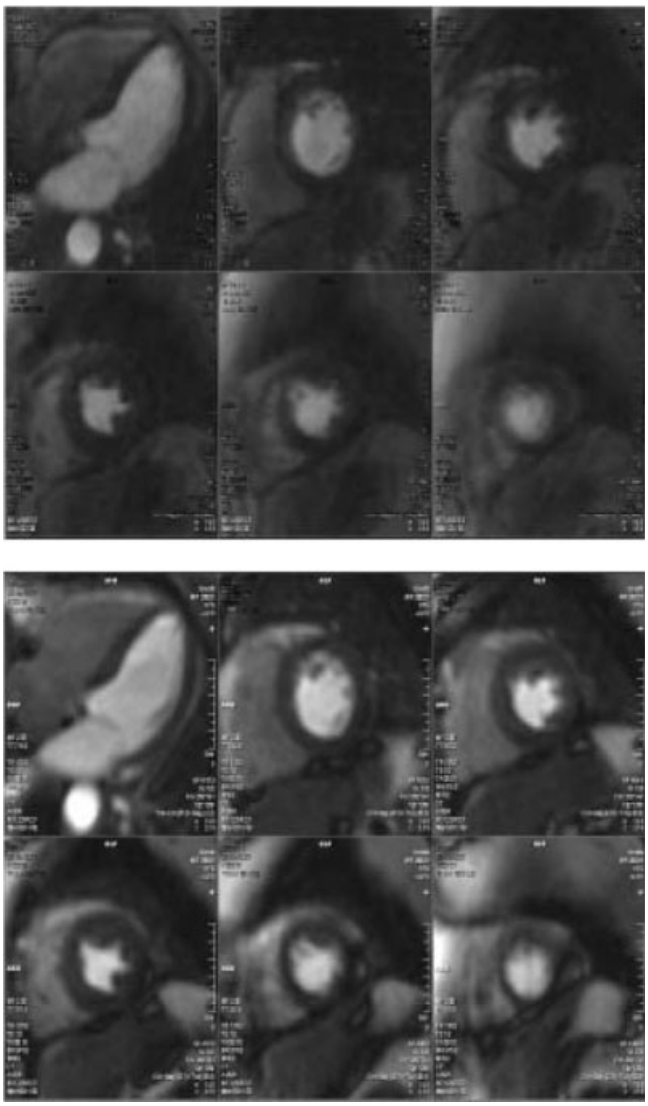

FIG. 5. Perfusion images at contrast reaches left ventricle from segmented EPI (upper six images) and SSFP (lower six images). Segmented EPI was used first, and SSFP was used 20 min later in this case.

cardium and blood pool. This is illustrated in Fig. 4, which shows in an example snapshot of one short-axis slice when contrast agent reaches the left ventricle (Fig. 4a), at maximal concentration in the left ventricle (Fig. 4b), and at maximal concentration in the myocardium (Fig. 4c), for both spoiled GRE (upper panel) and SSFP (lower panel), respectively. Likewise, Fig. 5 shows six slices with segmented EPI (upper panel) and partial Fourier SSFP (lower panel) at contrast arrival in the left ventricle. Although the TR of the SSFP perfusion sequence is slightly longer, fat appeared brighter and a dark susceptibility induced artifact was occasionally seen between myocardium and blood pool.

The average myocardial SNR for spoiled GRE was 24.1 ± 7.7 versus 42.6 ± 12.8 for SSFP, $P < 0.001$, while the average myocardial SNR for segmented EPI was 14.0 ± 4.2 versus 25.7 ± 9.3 for partial Fourier SSFP, $P = 0.013$, as shown in Fig. 6.

Average myocardial CNR for spoiled GRE was 124.3 ± 11.7 versus 153.1 ± 10.3 for SSFP, $P = 0.004$. Average myocardial CNR for segmented EPI was 107.2 ± 7.5 versus 158.6 ± 10.6 for partial Fourier SSFP, $P = 0.003$, as shown in Fig. 7.

The average myocardial relative maximal upslope for spoiled GRE was 10.3 ± 5.5 versus 10.1 ± 1.4 for SSFP, $P = 0.58$. The average myocardial relative maximal upslope for segmented EPI was 5.7 ± 0.6 versus 9.0 ± 0.4 for partial Fourier SSFP, $P = 0.001$, as shown in Fig. 8.

The SNR and CNR difference across all sequences consistently favored SSFP, while relative maximal upslope was comparable for spoiled GRE and SSFP and favored partial Fourier SSFP over segmented EPI.

DISCUSSION AND CONCLUSION

These results were obtained from resting perfusion images without pharmacological stress. SSFP perfusion images may show similar SNR and CNR improvement over spoiled GRE and segmented EPI in stress perfusion imaging. However, effects of motion and susceptibility artifacts associated with fast heart rates during stressing require further evaluation. Nevertheless, promising results have been reported from at least one preliminary study (22).

The data acquisition window we used ranged between 120 (segmented EPI) and 160 ms (spoiled GRE). We occasionally observed dark bands surrounding the left ventric-

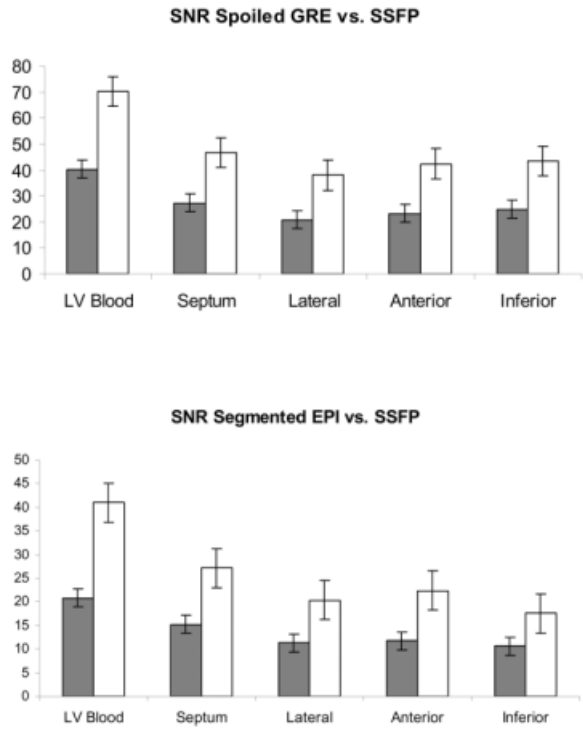

FIG. 6. SNR comparison SSFP versus spoiled GRE (upper graph) and SSFP versus segmented EPI (lower graph) by left ventricle and myocardial regions in volunteer studies. The average myocardial SNR for spoiled GRE was 24.1 ± 7.7 versus 42.6 ± 12.8 for SSFP, $P < 0.001$, while the average myocardial SNR for segmented EPI was 14.0 ± 4.2 versus 25.7 ± 9.3 for partial Fourier SSFP, $P = 0.013$.

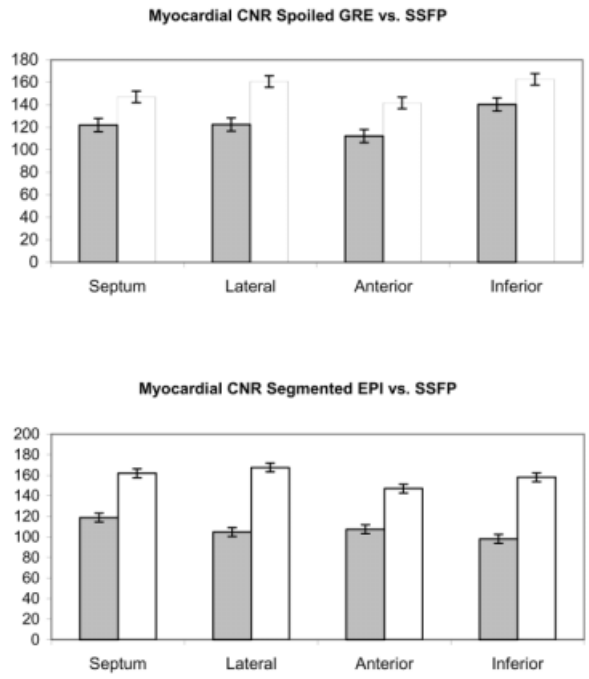

FIG. 7. Myocardial CNR comparison for SSFP versus spoiled GRE (upper graph) and SSFP versus segmented EPI (lower graph) by myocardial region in volunteer studies. Average myocardial CNR for spoiled GRE was 124.3 ± 11.7 versus 153.1 ± 10.3 for SSFP, $P = 0.004$. Average myocardial CNR for segmented EPI was 107.2 ± 7.5 versus 158.6 ± 10.6 for partial Fourier SSFP, $P = 0.003$.

ular blood pool, especially on images acquired during systole using a long data acquisition window. Such banding artifacts can be quite problematic as they can easily be confused with flow defects, especially when high spatial resolution imaging is used to depict regional subendocardial perfusion. These artifacts are not limited to SSFP images, but are more visible in SSFP images due to its higher CNR. The cause of this type of artifact has not been studied extensively, and the only reported solution is minimizing the data acquisition window (23).

One of the concerns often raised with regard to SSFP perfusion imaging is that since SSFP signal results from both T_1 and T_2 related effects, the T_2 contribution to the tissue contrast and the relative lower proportion of T_1 contribution than found with spoiled GRE or segmented EPI might compromise the detection of perfusion defects. Further studies are needed to address this issue.

In order to expedite the steady state of SSFP magnetization, 5 dummy $\alpha/2$ pulses were applied immediately prior to each data acquisition. Compared to 20 dummy pulses used the conventional inversion recovery SSFP sequence, fewer pulses were used because the improved contrast from the contrast agent in perfusion images shortens the time needed for the magnetization to reach steady state.

To avoid the coil sensitivity spatial variation effects, dynamic signals were commonly normalized by dividing averaged signal amplitude from the same areas before contrast arrival. However, the myocardial signal amplitude before contrast arrival is low due to the saturation pulse; the normalization may be subject to large variations. In our perfusion signal normalization, we used averaged signals of the same areas from all images before contrast arrival, since the signal before contrast agent is not totally annihilated, because of the use of saturation instead of inversion pulse.

We used two contrast injections on each volunteer study. The elimination half-lives of Omniscan is 77.8 ± 16 min (mean ± SD). To minimize the effect of residue contrast agent from the first injection to the second injection, we waited 20 min between two injections for contrast agent to wash out and randomized the order of study imaging sequence pair.

Both in vivo MRI compatible monitor (In vivo Research, Orlando, FL, USA) and Siemens Active Electrodes performed ECG triggering well when used in any of three sequences.

In summary, our results demonstrate that myocardial signal amplitude using the SSFP perfusion saturation recovery sequence demonstrates a linear relationship to contrast concentration within the dosage range used, while SSFP images consistently showed better SNR and CNR than spoiled GRE and segmented EPI, and relative myocardial upslope was greater with SSFP than with segmented EPI and similar for Spoiled GRE and SSFP. Further studies to evaluate SSFP stress perfusion imaging results and their relationship to quantitative coronary angiographic findings are required. Improved SNR in SSFP images may permit more reliable diagnostic stress perfusion

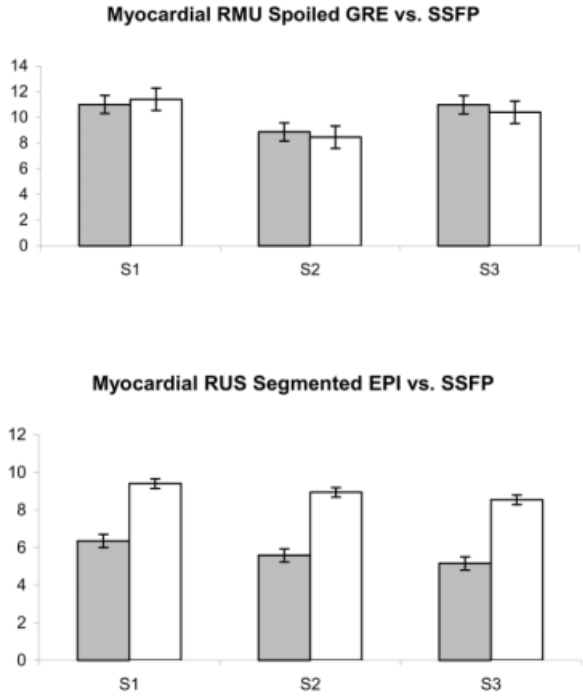

FIG. 8. Myocardial relative maximal upslope (RMU) comparison SSFP versus spoiled GRE (upper graph) and SSFP versus segmented EPI (lower graph) on three middle short axis slices (S1, S2, S3) in the volunteer study. The average myocardial relative maximal upslope for spoiled GRE was 10.3 ± 5.5 versus 10.1 ± 1.4 for SSFP, $P = 0.58$. The average myocardial relative maximal upslope for segmented EPI was 5.7 ± 0.6 versus 9.0 ± 0.4 for partial Fourier SSFP, $P = 0.001$.

imaging and improved myocardial blood flow quantification as well as further improvements in spatial coverage using parallel imaging (24).

The authors thank the Siemens cardiac MR development group in Chicago for their help, especially Drs. Orlando Simonetti and Qiang (Al) Zhang, as well as the teamwork of the entire St. Francis Hospital cardiac MR research group including Sunil Mathew, MD, Andressa Borges, MD, Williams Schapiro, RT, Kathy McGrath, RN, and Marguerite Roth, RN. The authors also thank James Goldfarb, PhD, for the valuable discussion and the preparation of the contrast agent doped phantom.

REFERENCES

1. Atkinson DJ, Burstein D, Edelman RR. First-pass cardiac perfusion: evaluation with ultrafast MR imaging. Radiology 1990;174:757–762.
2. Kramer CM, Rogers WJ, Geskin G, Power TP, Theobald TM, Hu YL, Reichek N. Usefulness of magnetic resonance imaging early after acute myocardial infarction. Am J Cardiol 1997;80:690–695.
3. Slavin G, Wolff S, Gupta S, Foo T. First-pass myocardial perfusion MR imaging with interleaved notched saturation: feasibility study. Radiology 2001;219:258–263.
4. Bertschinger KM, Nanz D, Buechi M, Luescher TF, Marincek B, von Schulthess GK, Schwitter J. Magnetic resonance myocardial first-pass perfusion imaging: parameter optimization for signal response and cardiac coverage. J Magn Reson Imaging 2001;14:556–562.
5. Jerosch-Herold M, Wilke N, Wang Y, Gong GR, Mansoor AM, Huang H, Gurchumelidze S, Stillman AE. Direct comparison of an intravascular and an extracellular contrast agent for quantification of myocardial perfusion. Cardiac MRI Group. Int J Cardiol Imaging 1999;15:453–464.
6. Edelman RR, Li W. Contrast-enhanced echo-planar MR imaging of myocardial perfusion: preliminary study in humans. Radiology 1994; 190:771–777.
7. Jerosch-Herold M, Huang H, Wilke N. Magnetization Prepared True FISP Myocardial Perfusion Imaging. In: Proceedings of the 7th Annual Meeting of ISMRM, Philadelphia, 1999. p 1882.
8. Wilke N, Kroll K, Merkle H, Wang Y, Ishibashi Y, Xu Y, Zhang J, Jerosch-Herold M, Muhler A, Stillman AE, et al. Regional myocardial blood volume and flow: first-pass MR imaging with polylysine-Gd-DTPA. J Magn Reson Imaging 1995;5:227–237.
9. Epstein FH, London JF, Peters DC, Goncalves LM, Agyeman K, Taylor J, Balaban RS, Arai AE. Multislice first-pass cardiac perfusion MRI: validation in a model of myocardial infarction. Magn Reson Med 2002; 47:482–491.
10. Fieno D, Jaffe W, Simonetti O, Judd R, Finn J. TrueFISP: assessment of accuracy for measurement of left ventricular mass in an animal model. J Magn Reson Imaging 2002;15:516–531.
11. Zhang Q, Crowe M, Chung YC, Simonetti OP. Acceleration techniques combined with TrueFISP for rapid first-pass myocardial perfusion imaging. In: Proceedings of the 11th Annual Meeting of ISMRM, Toronto, Canada, 2003. p 1655.
12. Schreiber WG, Schmitt M, Kalden P, Mohrs OK, Kreitner KF, Thelen M. Dynamic contrast-enhanced myocardial perfusion imaging using saturation-prepared TrueFISP. J Magn Reson Imaging 2002;16:641–652.
13. Deshpande VS, Shea SM, Laub G, Simonetti OP, Finn JP, Li D. 3D magnetization-prepared True-FISP: a new technique for imaging coronary arteries. Magn Reson Med 2001;46:494–502.
14. Haacke EM, et al. Magnetic resonance imaging: physical principles and sequence design. New York: Wiley; 1999.
15. Scheffler K. On the transient phase of balanced SSFP sequences. Magn Reson Med 2003;49:781–783.
16. Reeder SB, Atalar E, Faranesh AZ, McVeigh ER. Multi-echo segmented k-space imaging: an optimized hybrid sequence for ultrafast cardiac imaging. Magn Reson Med 1999;41:375–385.
17. Canet E, Douek P, Janier M, Bendid K, Amaya J, Millet P, Revel D. Influence of bolus volume and dose of gadolinium chelate for first-pass myocardial perfusion MR imaging studies. J Magn Reson Imaging 1995; 5:411–415.
18. Boos M, Scheffler K, Haselhorst R, Reese E, Frohlich J, Bongartz G. Arterial first pass gadolinium-CM dynamics as a function of several intravenous saline flush and Gd volumes. J Magn Reson Imaging 2001; 13:568–576.
19. Rusinek H, Lee V, Johnson S. Optimal dose of Gd-DTPA in dynamic MR studies. Magn Reson Med 2001;46:312–316.
20. Ishida M. The relation between injection rate and concentration of MR contrast medium in the heart and aorta: quantitative assement using multidector-row CT and double-syringe injection system. In: Proceedings of the 88th Scientific Assembly and Annual Meeting of RSNA, Chicago, 2002. p 1516.
21. Xu Y, Haacke E. Partial Fourier imaging in multi-dimensions: a means to save a full factor of two in time. J Magn Reson Imaging 2001;14:628–635.
22. Karg A, Oberholzer K, Abegunewardene N, Horstick G, Hoffmann N, Kreitner KF, Schreiber WG. Variation of the arterial input function in myocardial perfusion measurements: influence of ROI size and position. In: Proceedings of the 11th Annual Meeting of ISMRM, Toronto, Canada, 2003. p 1665.
23. Storey P, Chen Q, Li W, Edelman R, Prasad P. Band artifacts due to bulk motion. Magn Reson Med 2002;48:1028–1036.
24. Kellman P, Zhang Q, McVeigh ER, Arai AE, Simonetti OP. Accelerated true-FISP multi-slice first pass perfusion imaging using TSENSE. In: Proceedings of the 11th Annual Meeting of ISMRM, Toronto, Canada, 2003. p 1658.